AIP | Journal of Applied Physics

Suppression of low-temperature ferromagnetic phase in ultrathin FeRh films

G. C. Han, J. J. Qiu, Q. J. Yap, P. Luo, T. Kanbe et al.

Citation: J. Appl. Phys. **113**, 123909 (2013); doi: 10.1063/1.4798275
View online: http://dx.doi.org/10.1063/1.4798275
View Table of Contents: http://jap.aip.org/resource/1/JAPIAU/v113/i12
Published by the AIP Publishing LLC.

Suppression of low-temperature ferromagnetic phase in ultrathin FeRh films

G. C. Han,[1] J. J. Qiu,[1] Q. J. Yap,[1] P. Luo,[1] T. Kanbe,[2] T. Shige,[2] D. E. Laughlin,[3] and J.-G. Zhu[3]
[1]*Data Storage Institute, A*STAR, Republic of Singapore*
[2]*Showa Denko K.K, 13-9, Shiba daimon 1-Chome, Minato-ku, Tokyo 105-8518, Japan*
[3]*Data Storage Systems Center, Carnegie Mellon University, Pittsburgh, Pennsylvania 15213, USA*

(Received 7 January 2013; accepted 11 March 2013; published online 27 March 2013)

Highly ordered B2 FeRh films with sharp magnetic transitions from the antiferromagnetic (AF) to ferromagnetic (FM) states were prepared on thermally oxidized Si wafers with thicknesses as low as 10 nm. It is found that the transition temperature increases as the thickness decreases from 80 nm to 15 nm, and then decreases from 15 nm to 10 nm. While the ratio of the residual magnetization to the maximum magnetization keeps nearly unchanged for the film thickness of 15 nm and larger, it increases significantly when the thickness is reduced to 10 nm. This residual magnetization was suppressed by slightly increasing the Rh atomic content in 10 nm thick FeRh films. Low-pressure deposition is found to play an important role in the stabilization of the AF phase. By depositing FeRh films at an extremely low pressure of 0.057 Pa, a residual magnetization as small as 13.5 emu/cc at 100 K was observed for a film with a nominal thickness of 10 nm deposited on Si wafer. This value was further reduced to 6 emu/cc when the film is deposited on MgO substrates due to much improved FeRh crystallinity. These results are in close agreement with theoretical predictions on defect and interface induced FM stabilization. © *2013 American Institute of Physics*. [http://dx.doi.org/10.1063/1.4798275]

INTRODUCTION

B2 ordered FeRh alloys show a unique magnetic transition from the antiferromagnetic (AF) state at low temperature (LT) to the ferromagnetic (FM) state at elevated temperatures. This property has attracted increased interest in FeRh thin films due to its potential applications in magnetic random access memory (MRAM)[1,2] and magnetic recording media.[3,4] The main challenge for these applications is to prepare ultrathin FeRh films without a residual FM phase at LT and also that display a sharp transition to the FM state at elevated temperatures, and vice versa. As discussed in Ref. 3, FeRh layer with a thickness of 10 nm or less could provide sufficient exchange coupling strength between the storage layer and the assist layer to reduce switching field significantly without affecting the thermal stability of the storage layer at ambient temperature. However, a sharp AF-FM transition of FeRh film was only achieved in films with a thickness of 14 nm and above.[5] When the thickness was further reduced to 10 nm, a large residual magnetization was observed along with a broad transition.[6] Furthermore, the above mentioned films were grown on MgO (001) substrates, which cannot be utilized in practical applications. Some groups[7,8] have also reported the growth of FeRh films on amorphous substrates like glass and thermally oxidized Si substrates. However, a sharp transition was only achieved for thick films (~150 nm) using these substrates. The origin of the residual FM phase in the ultrathin film remains unclear. Fan *et al.*[9] ascribed the residual magnetization to the FM phase existing in a region within 6–8 nm of the FeRh near the top and/or bottom interfaces. Based on *ab initio* calculations, Lounis *et al.*[10] reported that a FM state is stable up to 9 atomic layers in an Rh-terminated FeRh film. In addition, the effects on the surface of the film accompanying the FeRh magnetostructural transition have been studied in Ref. 11, which shows that the surface strain relief fosters nucleation of the ferromagnetic phase.

In order to reduce the residual magnetization and understand its origin, systematic studies were performed on the magnetic properties of FeRh ultrathin (~10 nm) films grown on MgO(001) substrates and Si(001) substrates (with 1 μm thermal oxide). In comparison with the typical residual magnetization reported in literature (about 250 emu/cc),[6] the residual magnetization in this work was significantly reduced to 6 emu/cc through the fine tuning of the film composition and depositing the films at low pressure on MgO substrates.

EXPERIMENTS

FeRh thin films were grown on thermally oxidized Si (100) wafers by the co-sputtering of pure Fe and Rh targets in an ultrahigh vacuum sputtering system with a base pressure of $<5 \times 10^{-6}$ Pa. A typical layer structure is Si/SiO/MgO(10)/FeRh(10)/Ru(5), where the digital numbers indicate thicknesses of each layer in nanometers. The MgO seed layers and the Ru capping layers were both deposited at room temperature, while the FeRh films were deposited at a pressure of 0.059 Pa (unless specified otherwise) and a temperature of 650 °C. The film thicknesses were controlled by adjusting the deposition time with deposition rates obtained from the measured thicknesses and known deposition times of reference films which were deposited at room temperature. The crystalline structures of the films were analyzed by x-ray diffraction (XRD). X-ray photoelectron spectroscopy (XPS) was used to determine the film composition. Magnetic properties such as the temperature dependence of the magnetization and hysteresis loops were measured using a superconducting quantum interference device (SQUID) with a maximum field and a

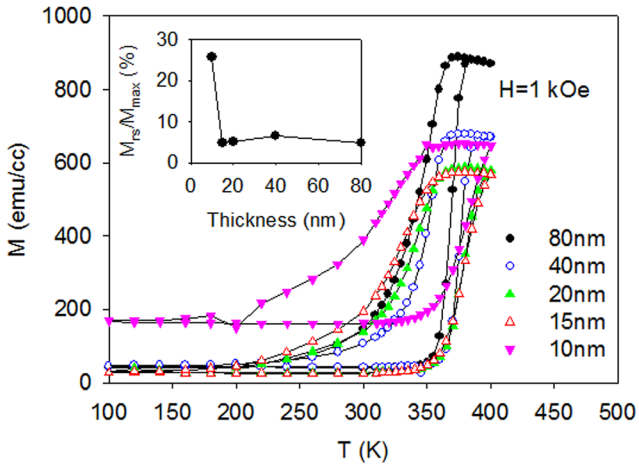

FIG. 1. Temperature dependence of magnetization measured at an applied field of 1 kOe as a function of film thickness. The inset gives the ratio of the residual magnetization (M_{min}) in the AF state to the maximum magnetization (M_{max}) achieved in the FM state for various thicknesses.

highest temperature of 70 kOe and 400 K, respectively. The composition was considered optimized when the sputtering powers were fixed at 80 W and 87.5 W for Fe and Rh targets, respectively, to produce a smallest residual magnetization at 100 K for a 80 nm thick FeRh film.

RESULTS AND DISCUSSION

Fig. 1 shows the temperature dependence of the magnetization (M-T) with an applied field of H = 1 kOe for various thicknesses of FeRh layers. All these films clearly show an AF-FM phase transition. As the thickness decreases, the maximum magnetization achieved at 400 K after heating decreases and the transition hysteresis becomes broader, which is consistent with that reported in the literature.[6] It is noted that although the hysteresis of the transition temperatures defined by the maximum derivative of the M-T curves for the 80 nm thick film is about 20 K, similar to that reported before,[5,6] there is a long tail for the FM-AF transition down to a temperature below 300 K. This broadening of the FM-AF transition could be attributed to the composition fluctuations in the film as well as the poorer crystalline orientations of the MgO buffer layers grown on the oxidized Si wafers as compared to MgO(001) substrates. Similar to that reported by Suzuki *et al.*,[6] the AF-FM transition temperature increases slightly as the film thickness decreases from 80 nm to 15 nm as observed in Fig. 1. This could be ascribed to the stress induced by the lattice–mismatch at the interface between FeRh and MgO, analogous to the observation in high-pressure experiments on bulk FeRh.[12,13] However, one can see the transition temperature is shifted to the lower temperature when the thickness is reduced from 15 nm to 10 nm, which will be discussed later. As shown in the inset of Fig. 1, it is found that the ratio of the residual magnetization (M_{rs}) in the AF state to the maximum magnetization (M_{max}) achieved in the FM state remains nearly unchanged at about 4.5% as the thickness decreases from 80 nm to 15 nm. This result implies that this residual magnetization is not from the interface, but from the composition fluctuations throughout the film. When the thickness was further reduced from 15 nm to 10 nm, the residual magnetization increases significantly, together with an increase in the total magnetization achieved at the FM state. The increase of the residual magnetization at the ultrathin thickness has been ascribed to the surface/interface effect due to the broken symmetry which contracts the 4 d band of the Rh atoms, increasing the density of states at the Fermi level [Ref. 10]. However, since the increase in residual magnetization is accompanied by an increase in the total magnetization at the FM state and the film thickness is much larger than that for the FM stabilization, we think the residual FM phase might arise from the formation of FM α' phase due to the composition fluctuations over the film.

In order to reduce the FM α' phase in the ultrathin FeRh film, the composition of the film was further tuned at a film thickness of 10 nm. To do this, the sputtering power of the Fe target was fixed at 80 W, while Rh sputtering power (P_{Rh}) was increased gradually. As shown in Fig. 2, a slight increase of the Rh content reduces the residual magnetization significantly, which is most likely due to the suppression of the α' phase or the transformation from the FM α' phase to the AF α'' phase. A small residual magnetization of about 18 emu/cc was obtained when $P_{Rh} = 92.5$ W and 95 W. In contrast, Suzuki *et al.*[6] reported a residual magnetization of 250 emu/cc for a 10 nm thick FeRh film. As reported by van Driel *et al.*,[14] Rh richer FeRh films have higher transition temperature and lower saturation magnetization. When the Rh content is further increased to $P_{Rh} = 97$ W, as shown by filled downward triangles in Fig. 2, the residual magnetization increases along with a reduced magnetization after the AF-FM transition occurs at about 400 K. As shown in Fig. 3, XRD results show no sign of the γ FeRh phase in the films as the sputtering power of Rh increases from 87.5 W to 97 W. The background difference in XRD measurements for the sample deposited at 92.5 W resulted from the different alignment of XRD during θ-2θ scans. This result suggests that the thinner film needs more Rh to stabilize the AF phase than the thicker films. The additional Rh does not promote the formation of γ FeRh phase, but most likely forming Rh-terminated grains. The AF stabilization in the Rh-terminated grains seems to contradict the results based on the *ab initio*

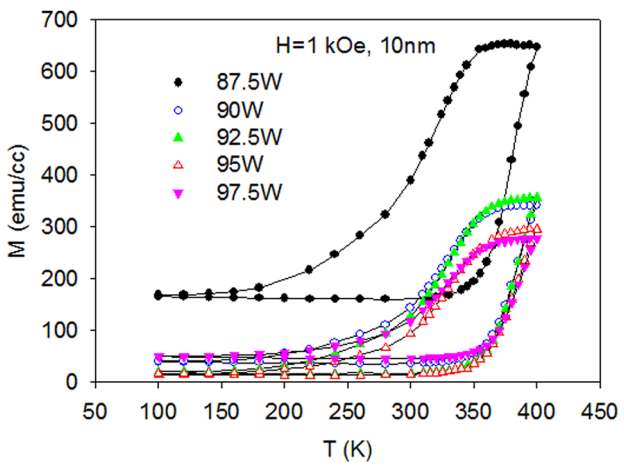

FIG. 2. M-T curves of 10 nm thick films deposited with different sputtering powers for Rh target for the fine tuning of Rh content in the films.

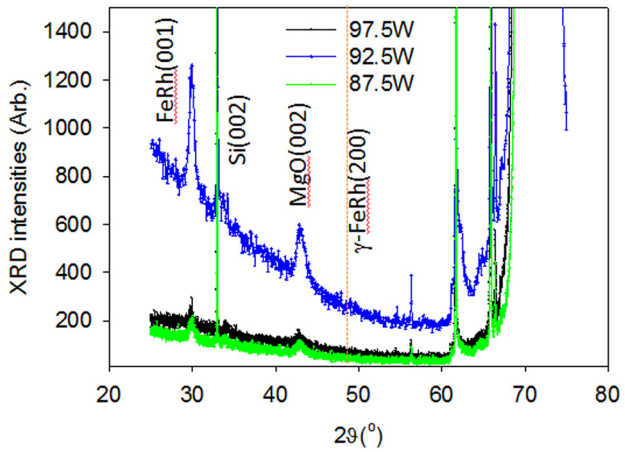

FIG. 3. XRD patterns of 10 nm thick B2 ordered FeRh films with different Rh contents. No γ FeRh (200) peak is observed, indicating that there is no γ FeRh phase formation even in the Rh-rich film.

calculations,[10] which show that the AF phase is more stable than the FM phase at any thickness for the Fe-terminated film while the FM phase will be more stable only till 9 atomic layers for the Rh-terminated film. However, it should be pointed out that the calculations in Ref. 10 did not consider the interaction (FM exchange coupling) between FeRh grains in a real film. For Rh-terminated grains, the FM exchange coupling could be decoupled by Rh layer, thus stabilizing the AF arrangement within the grain. The exchange coupling induced FM stabilization could be demonstrated in the following result. As shown in Fig. 4, when a FM Fe layer was deposited on the FeRh layer before Ru capping layer at room temperature (to avoid the interdiffusion between the Fe layer and FeRh layer), the AF-FM transition in the film was completely destroyed. In contrast, for Ru capped FeRh films deposited subsequently, a clear AF-FM transition was observed. Similarly, Ding *et al.*[15] also reported that the near-surface/interfacial magnetism of FeRh may be modified by choice of capping layer. They found that even a non-magnetic capping layer could induce FM stabilization in the FeRh film.

Our sputtering system is equipped with an inductively coupled plasma coil which allows for thin film deposition at an extremely low pressure down to 0.057 Pa. As discussed above, our ultrathin FeRh films exhibited lower residual magnetization and sharper transitions than reported so far in literature. To examine whether the good FeRh performance results from the low-pressure deposition or not, the magnetic properties of two samples deposited at a pressure of 0.105 Pa and 0.057 Pa were studied. At 0.105 Pa, the composition was tuned and considered optimum when the lowest residual magnetization was achieved. At 0.057 Pa, the composition was adjusted to be the same as the optimum composition achieved at 0.105 Pa. Thus, the effects arising from composition difference are excluded when comparing the properties of these two samples. XPS measurements (not given here) confirmed that the two samples have exactly the same Fe and Rh content. Fig. 5 shows M-T curves measured at 1 kOe (the inset) and 50 kOe. At an applied field of 1 kOe, as shown in the inset of Fig. 5, the AF-FM transition is not yet completed as SQUID can only heat the sample up to 400 K. An complete transition can be only observed at a high magnetic field. As shown in Fig. 5, when a field of 50 kOe was applied, the transition is shifted below 400 K. As a result, the larger magnetic transition was obtained and the magnetization at 400 K is much larger than that measured at 1 kOe. At a field of 50 kOe, not only was a small residual magnetization obtained, a sharp AF-FM transition was also observed for the sample deposited at 0.057 Pa, while the sample deposited at higher pressure shows a broader transition with a larger residual magnetization. Such a small residual magnetization in the low-pressure deposited sample was further confirmed through magnetization curve (M-H) measurements. Figs. 6(a) and 6(b) show M-H curves measured at 100 K, 300 K, and 400 K for the samples deposited at pressures of 0.105 Pa and 0.057 Pa, respectively. For the FeRh film deposited at the pressure of 0.105 Pa, obvious FM hysteresis loops were observed at a temperature down to 100 K, while almost no hysteresis loop was detected at 300 K for the sample deposited at the pressure of 0.057 Pa. However, it is also noted that at 100 K there is a small hysteresis loop for the low-pressure deposited sample, showing the existence of the FM phase. A careful examination of the M-T curve measured at 1 kOe for

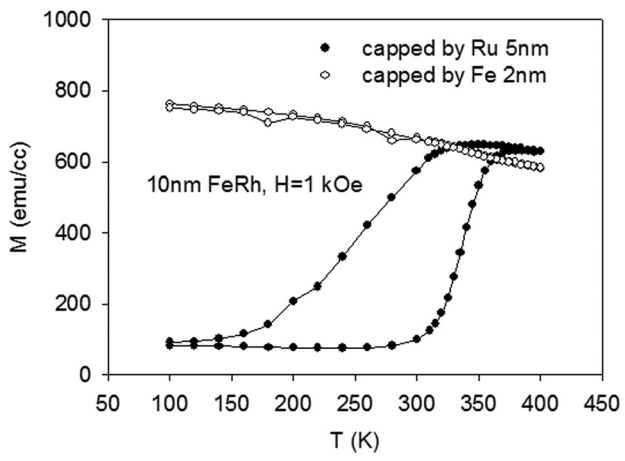

FIG. 4. M-T curves of 10 nm thick films capped by Fe (2 nm) and Ru (5 nm).

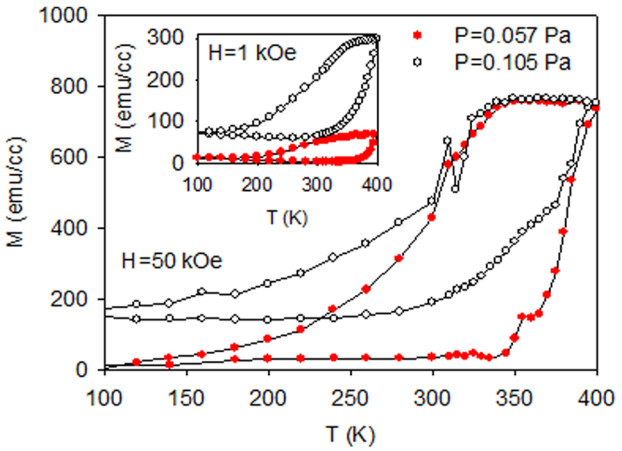

FIG. 5. M-T curves of 10 nm thick films deposited at different pressures measured at a field of 50 kOe. The inset gives the M-T curves measured at a field of 1 kOe.

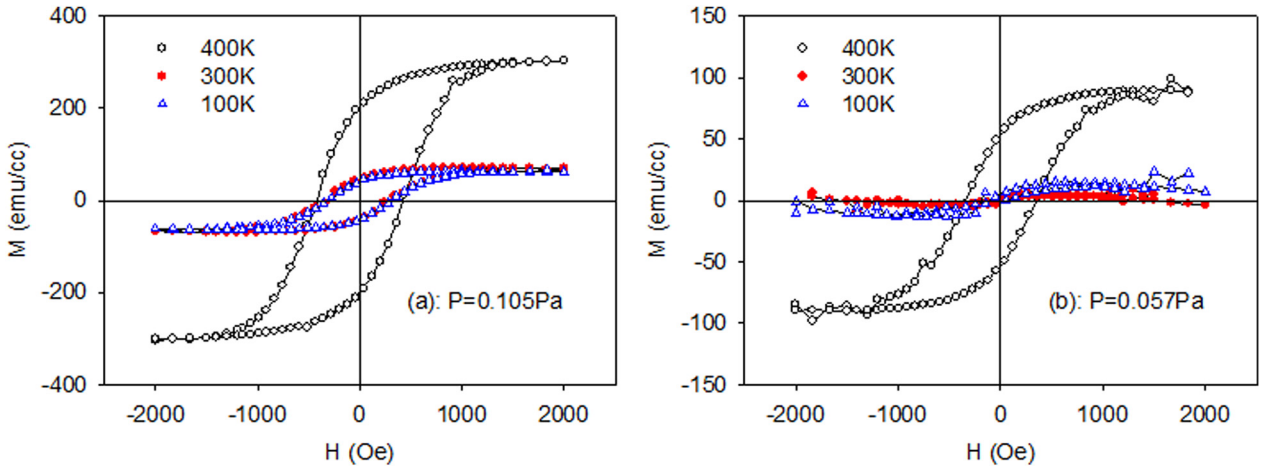

FIG. 6. Magnetization hysteresis loop of 10 nm thick FeRh films deposited at (a) 0.105 Pa and (b) 0.057 Pa measured at various temperatures.

the low-pressure sample shows that the magnetization decreases almost linearly from 13.5 emu/cc to 3 emu/cc as temperature increases from 100 K to 260 K before the onset of the AF-FM transition. Extrapolating this linear M-T curve to zero magnetization, we found that the Curie temperature of this FM phase is about 310 K. As the composition was considered optimized, this FM phase could be ascribed to the interface/surface induced FM stabilization as predicted by Fan *et al.*[9] and Lounis *et al.*[10] Comparing the XRD results (not shown here) of these two samples, it was observed that the two samples have similar diffraction peaks in θ-2θ scans and the resulting order parameter is also similar ($I_{001}/I_{002} = 0.94$ and 0.98 for P = 0.057 Pa and 0.105 Pa, respectively). Therefore, it is most likely that the smaller residual magnetization and the sharper transition observed for the film deposited at low pressure is from the more uniform composition distribution in the film which resulted from the higher energy of the sputtered adatoms arriving on the substrate due to the lower working pressure. In addition, as shown in Fig. 7, the grains in the film deposited at low-pressure pack more closely and are slightly larger in size. This could lead to an improvement in the strength of the magnetic coupling between the grains, which might be another reason for the sharper transition observed in Fig. 5.

It is noted that a certain amount of residual magnetization appears for all of our samples. Moreover, at a thickness of 10 nm, the transition is much broader than that in thicker films. From the phase diagram,[16] it can be seen that the transition temperature is expected to increase as Rh content increases within the α'' phase region. Hence, a FeRh film having a continuous composition spread within the α'' phase could correspondingly result in the onset of AF-FM transition occurring at a continuous spread of temperatures, thus possibly explaining the broadening of AF-FM transition. It is noted here that given the nature of the co-sputtering process, it is reasonable to expect some composition distribution in the deposited films. Other possible mechanisms responsible for the broadening include stress and defects. As pointed out by Kaneta *et al.*,[17] the AF structure would be destabilized when the amount of the site-exchange defect density exceeds the threshold of 0.8%/f.u. In order to examine this effect, MgO(001) substrate was used to grow an ultrathin (10 nm) FeRh films to improve the crystallinity. For comparison, a Si/SiO substrate was also loaded in the chamber in order to deposit the FeRh film simultaneously on both substrates. An MgO buffer layer was deposited on both substrates before the FeRh deposition. The M-T curves of the two samples are shown in Fig. 8. The magnetic transition is much sharper and

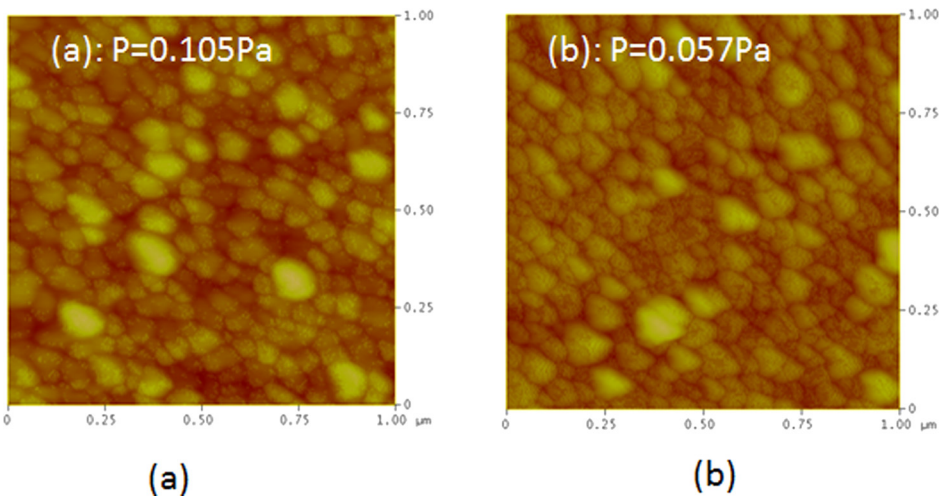

FIG. 7. AFM images of 10 nm thick FeRh films deposited at different pressures: (a) 0.105 Pa and (b) 0.057 Pa.

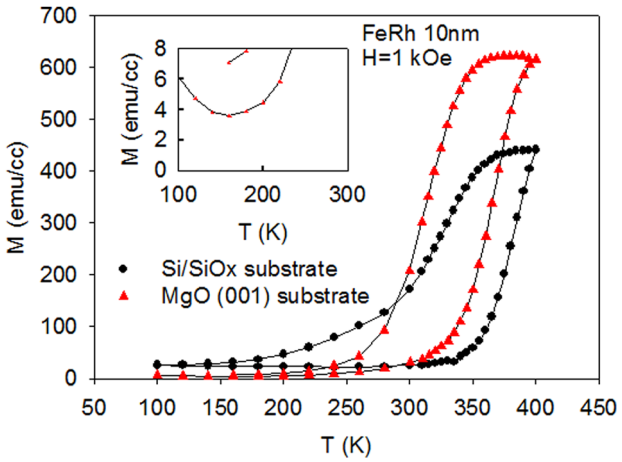

FIG. 8. M-T curves for 10 nm thick FeRh films deposited on MgO and Si/SiO substrates. The inset shows the enlarged M-T curves at low temperatures.

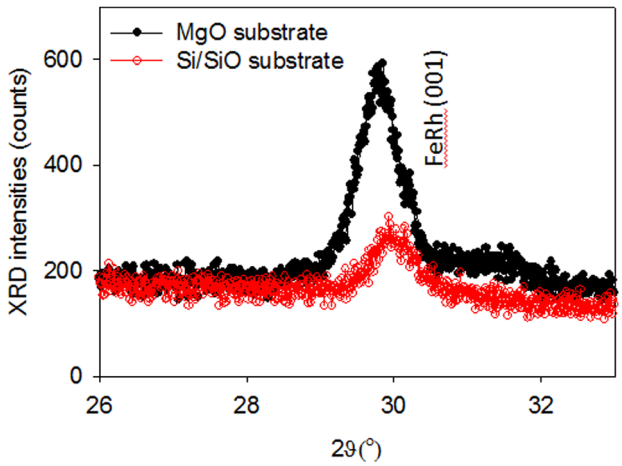

FIG. 9. XRD FeRh (001) peaks for samples deposited on Si/SiO wafer and MgO substrate.

the amplitude of magnetization transition was found to be larger for the film deposited on MgO substrate. The temperature hysteresis of the transition is 56 K and 60.6 K for the MgO and Si substrates, respectively. The hysteresis of the transition is much larger than that observed in thicker films, even for the MgO substrate. Such behavior was attributed to the decrease of the grain size in the ultrathin films.[18] The stress and its distribution in the film could be another origin of the broader transition observed in the FeRh film grown on Si substrate. On the other hand, for the film grown on MgO substrate, the stress could be more uniform over the surface due to better crystalline structure of the MgO underlayer. In other words, the FeRh layer deposited on Si substrate might have a wider crystalline orientation distribution of FeRh lattice. That could cause a large distribution of the stress from the lattice mismatch between FeRh and MgO buffer layer, resulting in the broader transition. It is noted that for the FeRh film deposited on the MgO substrate, the residual magnetization is as small as 6 emu/cc at 100 K, in contrast to 24 emu/cc for the film deposited on Si/SiO wafer, implying the high stability of the AF phase at low temperatures for the former. Such low residual magnetization and sharp transition could be related to a high quality crystalline structure of the FeRh film. As shown in Fig. 9, the intensity of FeRh (001) XRD peak is much higher for the film deposited on the MgO substrate and this in addition to its narrow width indicates a much better crystalline structure in the FeRh film deposited on MgO, since the two samples were deposited simultaneously and the thickness of the films is exactly the same. This suggests that the good magnetic properties could be achieved by improving the crystalline ordering of ultrathin FeRh films. However, as shown in the inset of Fig. 8, even the FeRh film on MgO substrate still exhibits some residual magnetization which decreases as temperature increases from 100 K to 160 K, clearly demonstrating the existence of a FM phase. This FM phase might be attributed to the defect-induced FM stabilization. Further suppression of the residual magnetization could require a complete removal of the defects in the film.

As shown in Fig. 9, the FeRh (001) peak is shifted to the lower angle for the film deposited on MgO substrate, implying the expansion of the film along c axis. The lattice parameter c of FeRh films is estimated to be 2.984 and 2.999 Å for Si and MgO substrates, respectively. This is similar to the result reported by Bordel *et al.*,[19] where FeRh grown on an ion-beam-assist-deposited MgO layer on a-SiO_x/Si substrate was found to have a smaller c compared to FeRh grown on regular MgO substrates. The larger c parameter in FeRh grown on single crystalline MgO substrates is attributed to the in-plane contraction along the [100] and [010] axes due to the lattice mismatch between the FeRh film and the MgO substrate. This compressive stress would increase the magnetic transition temperature,[12,13] which is contrary to the observation from Fig. 8. AFM images of the films (not given here) did not show much difference in the surface morphology of the two films. It is unclear why the transition temperature is lower for the FeRh film grown on MgO substrate. The large difference in the thermal expansion coefficients between Si (4.68×10^{-6}/K) and MgO (13.5×10^{-6}/K) substrates might also have caused the variation in the transition properties. Since the thermal expansion coefficient of MgO substrate is larger, greater compressive stress might be produced in the FeRh film when the FeRh film deposited at 650 °C was cooled down to room temperature. The resultant effect could be such that the transition temperature of the FeRh film grown on MgO substrate is further increased. From the literature[19,20] and the results shown in Fig. 1, the transition of the thicker (>15 nm) FeRh films is always shifted towards higher temperatures as the compressive stress in the film increases or is expected to increase, whereas for thinner films (10 nm), the transition always moved towards lower temperatures as reported in Refs. 6 and 21, and shown in Fig. 1. This suggests that the effect of the stress on the AF-FM transition could be different for thicker and thinner films. Because films typically relax stress by nucleating defects, a higher stress in thinner films will generally lead to more defects, which would stabilize the FM state at lower temperatures and thus lower the AF-FM transition temperature. A similar defect effect was reported by irradiation experiments using electron and heavy ions.[22,23] While electron irradiation decreases the transition temperature by 3–18 K without changing the B2 crystalline structure,

the ion irradiation induces the FM stabilization (no AF-FM transition was observed down to 5 K).

CONCLUSION

In summary, systematic studies of ultrathin FeRh films were carried out to achieve good performance of magnetic transition properties. The sharp magnetic transitions and small residual magnetizations were achieved by optimizing the composition and depositing the films at an extremely low pressure. It is demonstrated that the residual magnetization of the ultrathin FeRh film are not only sensitive to the composition and its distribution, the crystalline ordering and granular structure, but also to the applied field and the interaction with the capping layer. Using Ru as the capping layer, residual magnetizations as small as 13.5 emu/cc and 6 emu/cc at 100 K were observed for 10 nm thick films deposited on oxidized Si wafer and MgO(001) substrate, respectively. These results suggest that the FeRh films could be promising for practical applications in recording media and MRAM.

[1]E. Fullerton, S. Maat, and J. U. Thiele, U.S. patent 20050281081 (2005).
[2]J.-G. Zhu, Y. Luo, and X. Li, U.S. patent 7,826,258 (2010).
[3]J.-G. Zhu and D. E. Laughlin, U.S. patent, US2005/0281081A1 (2005).
[4]J. Thiele, S. Maat, and E. E. Fullerton, Appl. Phys. Lett. **82**, 2859 (2003).
[5]D. Kande, S. Pisana, D. Weller, D. E. Laughlin, and J. G. Zhu, IEEE Trans. Magn. **47**, 3296 (2011).
[6]I. Suzuki, T. Koike, M. Itoh, T. Taniyama, and T. Sato, J. Appl. Phys. **105**, 07E501 (2009).
[7]J. M. Lommel, J. Appl. Phys. **37**, 1483 (1966).
[8]S. Hashi, S. Yanase, Y. Okazaki, and M. Inoue, IEEE Trans. Magn. **40**, 2784 (2004).
[9]R. Fan, C. J. Kinane, T. R. Charlton, R. Dorner, M. Ali, M. A. de Vries, R. M. D. Brydson, C. H. Marrows, B. J. Hickey, D. A. Arena, B. K. Tanner, G. Nisbet, and S. Langridge, Phys. Rev. B **82**, 184418 (2010).
[10]S. Lounis, M. Benakki, and C. Demangeat, Phys. Rev. B **67**, 094432 (2003).
[11]J. W. Kim, P. J. Ryan, Y. Ding, L. H. Lewis, M. Ali, C. J. Kinane, B. J. Hickey, C. H. Marrows, and D. A. Arena, Appl. Phys. Lett. **95**, 222515 (2009).
[12]L. I. Vinokurova, A. Vlasov, N. Kulikov, and M. Pardavi-Horváth, J. Magn. Magn. Mater. **25**, 201 (1981).
[13]A. Hernando, J. M. Barandiarán, J. M. Rojo, and J. C. Gómez-Sal, J. Magn. Magn. Mater. **174**, 181 (1997).
[14]J. van Driel, R. Coehoorn, and G. J. Strijkers, J. Appl. Phys. **85**, 1026 (1999).
[15]Y. Ding, D. A. Arena, J. Dvorak, M. Ali, C. J. Kinane, C. H. Marrows, B. J. Hickey, and L. H. Lewis, J. Appl. Phys. **103**, 07B515 (2008).
[16]T. B. Massalski, *Binary Alloy Phase Diagrams* (ASM International, Materials Park, OH, 1992), Vol. 2, p. 1760.
[17]Y. Kaneta, S. Ishino, Y. Chen, S. Iwata, and A. Iwase, Jpn. J. Appl. Phys., Part 1 **50**, 105803 (2011).
[18]Y. Ohtani and I. Hatakeyama, J. Magn. Magn. Mater. **131**, 339 (1994).
[19]C. Bordel, J. Juraszek, David W. Cooke, C. Baldasseroni, S. Mankovsky, J. Minár, H. Ebert, S. Moyerman, E. E. Fullerton, and F. Hellman, Phys. Rev. Lett. **109**, 117201 (2012).
[20]S. Maat, J.-U. Thiele, and E. E. Fullerton, Phys. Rev. B **72**, 214432 (2005).
[21]J.-U. Thiele, S. Maat, J. L. Robertson, and E. E. Fullerton, IEEE Trans. Magn. **40**, 2537 (2004).
[22]M. Fukuzumi, Y. Chimi, N. Ishikawa, F. Ono, S. Komatsu, and A. Iwase, Nucl. Instrum Methods B **230**, 269 (2005).
[23]M. Fukuzumi, R. Taniguchi, S. Komatsu, F. Ono, A. Iwase, Mater. Res. Soc. Symp. Proc. **792**, 393 (2004).